

Article

C–H...X (X = F, Cl, Br, I) Versus π -Stacking in the Crystal Packing of Compounds Containing the $\{M(\text{tpy})X_3\}$ Motif

Catherine E. Housecroft * and Edwin C. Constable 

Department of Chemistry, University of Basel, BPR 1095, Mattenstrasse 22, Postfach, 4002 Basel, Switzerland; edwin.constable@unibas.ch

* Correspondence: catherine.housecroft@unibas.ch

Abstract: Analysis of the data in the Cambridge Structural Database (CSD) for compounds containing an $\{M(\text{tpy})X_3\}$ motif (tpy = 2,2':6',2''-terpyridine, M = any metal, X = F, Cl, Br, I) reveals 17 isostructural mononuclear $[M(\text{tpy})X_3]$ compounds crystallizing without lattice solvent; both face-to-face π -stacking of pyridine rings and C–H3/H3'...X hydrogen bonding appear to be equally important. Regardless of coordination number (CN = 6, 7 or 8) and nuclearity (mono- or dinuclear), a recurring packing feature in other compounds containing an $\{M(\text{tpy})X_3\}$ unit is the presence of bifurcated Cl...H3/H3' interactions, complemented in some cases by Cl...H5'/H3'' interactions, consistent with the acidic H3, H3', H5', and H3'' atoms of a coordinated tpy ligand. Octahedral $[M(\text{tpy})F_3]$ complexes crystallize as hydrates with strong F...H–OH hydrogen bonding dominating the crystal packing.

Keywords: metal complexes; 2,2':6',2''-terpyridine; $[M(\text{tpy})X_3]$; C–H...X interactions; crystal packing



Citation: Housecroft, C.E.; Constable, E.C. C–H...X (X = F, Cl, Br, I) Versus π -Stacking in the Crystal Packing of Compounds Containing the $\{M(\text{tpy})X_3\}$ Motif. *Crystals* **2023**, *13*, 885. <https://doi.org/10.3390/cryst13060885>

Academic Editor: Jesús Sanmartín-Matalobos

Received: 9 May 2023

Revised: 23 May 2023

Accepted: 26 May 2023

Published: 28 May 2023

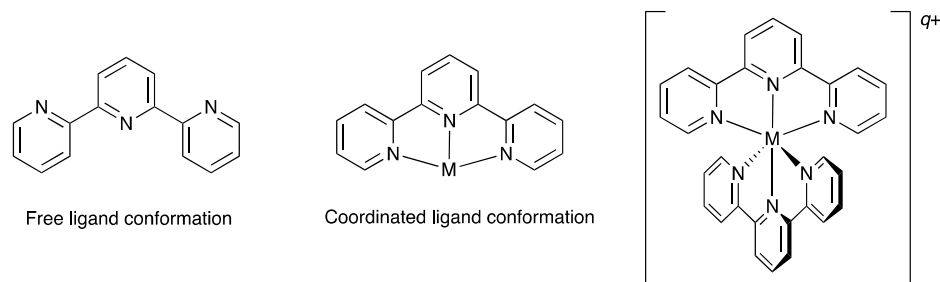


Copyright: © 2023 by the authors. Licensee MDPI, Basel, Switzerland. This article is an open access article distributed under the terms and conditions of the Creative Commons Attribution (CC BY) license (<https://creativecommons.org/licenses/by/4.0/>).

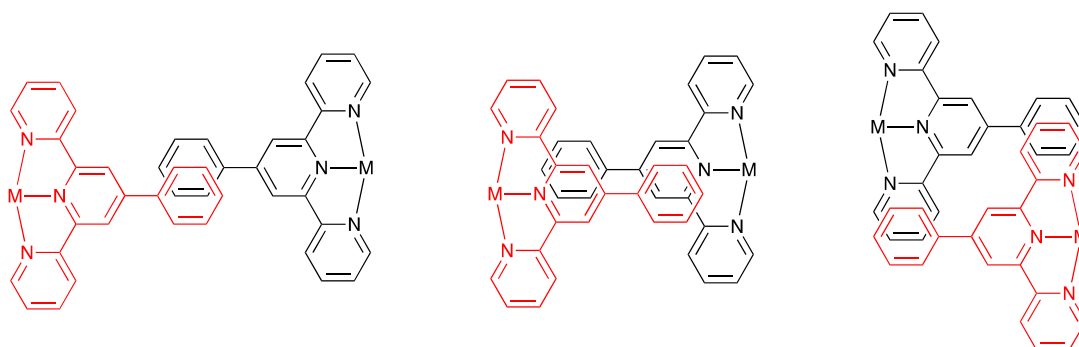
1. Introduction

The ligand 2,2':6',2''-terpyridine (tpy) typically coordinates to metal ions in a terdentate, bis-chelating mode with a concomitant conformational change from *s-trans,s-trans* to *s-cis,s-cis* (Scheme 1). Mononuclear six-coordinate complexes of the type $[M(\text{tpy})_2]^{q+}$ ($q \geq 0$) and $[M(\text{tpy})X_3]^{q\pm}$ ($q \geq 0$) are common [1–4], and complexes with higher coordination numbers are known with larger metal ions, such as those from the *f*-block. Solid-state packing interactions between $\{M(\text{tpy})_2\}$ cations have been the focus of detailed investigations by McMurtie and Dance [5–7]. Offset-face-to-face (OFF) and edge-to-face (EF) interactions between pyridine rings are a recurring feature, and the introduction of a 4'-aryl substituent introduces an additional π -stacking motif leading to the embraces shown in Scheme 2 [5]. The offset arene...arene contacts displayed in Scheme 2 are typical packing arrangements, not only in tpy-containing compounds but also in the solid-state structures of many metal coordination compounds containing aromatic nitrogen-donor ligands [8]; in 2009, Dance and Scudder highlighted their role in molecular crystals [9]. These authors recognized and defined a quadruple aryl embrace (QAE) as the fundamental packing interaction present in the chiral, hexagonal motif that is a recurring feature in salts of $[M(\text{bpy})_3]^{q+}$ (bpy = 2,2'-bipyridine) complexes. More recently, using data from the Cambridge Structural Database (CSD) [10], we demonstrated the significance of short contacts between atoms H3 and H3' of the bpy ligands in $[M(\text{bpy})_3]^{q+}$ and the counterion (see Scheme 3 for atom numbering) which may be augmented by interactions of the anion with bpy atoms H4 and H5. This combination of CH...X contacts results in anions residing either in the center or lying above and/or below the centroid of the hexagonal $\{M(\text{bpy})_3\}_6$ motif [11,12]. We extended these investigations to octahedral *cis*- $[M(\text{bpy})_2X_2]$ coordination compounds and showed that a recurrent packing motif is a dimeric unit containing $\text{CH}_{\text{bpy}}\dots\text{X}$ contacts and intermolecular face-to-face π -stacking of bpy ligands; in some cases, $\text{CH}_{\text{bpy}}\dots\text{X}$ contacts are the dominant features of the crystal-packing [13]. With this latter observation in mind, we turned our attention to $[M(\text{tpy})X_3]^{q\pm}$ ($q \geq 0$) complexes in which X = F, Cl,

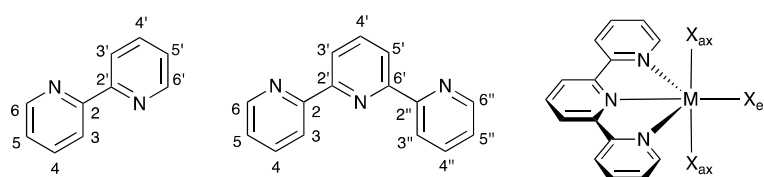
Br, or I. As with bpy, the H3 and H3' atoms of a coordinated tpy ligand are acidic [14], and we were interested in exploring whether the solid-state structures of compounds containing $\{M(\text{tpy})X_3\}$ domains showed intermolecular CH...X interactions with these atoms. Herein, we describe the patterns in crystal packing that are found in complexes of the type $[M(\text{tpy})X_3]^{q\pm}$ ($q \geq 0$). Structural data for this article have been retrieved from the CSD [10] (see the Methods Section).



Scheme 1. Representations of tpy in the *s-trans,s-trans* conformation found in the free ligand, the change to an *s-cis,s-cis* conformation upon metal coordination, and in an octahedral $[M(\text{tpy})_2]^{q+}$ complex.



Scheme 2. Three possible embraces of two $\{M(4'\text{-Phtpy})\}$ units (4'-Phtpy = 4'-phenyl-2,2':6',2''-terpyridine); these are described in reference [5].



Scheme 3. Structures of the free ligands bpy and tpy with atom numbering and a schematic representation of the structure of *mer*- $[M(\text{tpy})X_3]$ showing the axial (ax) and equatorial (eq) halogenido ligands, X; the three nitrogen donor atoms together with X_{eq} define a mean plane. In complexes containing unsubstituted terdentate tpy ligands, H3 and H3'' are equivalent, as are H3' and H5'.

2. Methods

Conquest (version 2022.3.0 including November 2022 updates) [15] was used to search the CSD [10] for compounds containing $\{M(\text{tpy})X_3\}$ motifs (M = any metal = '4M' in Conquest; X = any halogen). The H atoms of the tpy ligand were explicitly defined, thereby excluding functionalized tpy ligands. The inter-ring C–C bonds in the tpy ligand and the M–N and M–X bonds were specified as being of “any type” in Conquest [15]. The connectivity of the M and X atoms were not constrained. In the text, the abbreviation CN is used for coordination number. Analysis of the structures was carried out using the program Mercury (version 2022.3.0) [16]. In structures in which the H atom coordinates were not

available, H positions were added in Mercury [16]. All H positions were normalized in Mercury, with C–H = 1.089 Å. The settings in Mercury for a ‘short contact’ (sum of the van der Waals radii + 0.1 Å) were applied to identify H...X interactions. Disordered structures were included in the analysis.

3. Defining the Sets of Structures for Analysis

The search of the CSD defined in Section 2 resulted in 51 hits. The compounds with CSD refcodes EXODAX and EXODEB are polymeric [17], and those with refcodes SUSKUO [18] and VAFDUD [19] contain multinuclear species. $[\text{Pb}_3(\text{tpy})_3\text{Br}_2(\mu\text{-Br})_2(\mu_3\text{-Br})_2]\cdot 2\text{H}_2\text{O}$ (refcode RAQQII) contains a trinuclear core [20], while the compounds with refcodes HOBXIG and ELORAZ contain $[\text{Bi}(\text{tpy})_2\text{I}_2]^+$ and $[\text{Bi}_2(\text{tpy})\text{I}_4(\mu\text{-I})_3]^-$, and $[\text{Bi}(\text{tpy})_2\text{I}_2]^+$ and $[\text{Bi}(\text{tpy})\text{I}_4]^-$ ions, respectively [21,22]. These seven structures were excluded from detailed analyses.

The remaining 44 solid-state structures fell into categories of mononuclear (33) and dinuclear (11) species, including several redeterminations at either the same or different temperatures. We consider these groups of structures separately in the following discussion. In the absence of additional ligands, the $\{\text{M}(\text{tpy})\text{X}_3\}$ moiety (in both mononuclear and dinuclear complexes) is typically octahedral (or, more correctly, pseudo-octahedral) and constrained to a *meridional* arrangement of the three nitrogen donors of the tpy. The three halogenido ligands are concomitantly in an orthogonal *meridional* arrangement (Scheme 3). Accordingly, there are two chemically and structurally distinct types of halogen atoms—two axial ligands (ax) and one equatorial ligand (eq), with the axis orthogonal to the mean plane of the tpy ligand (Scheme 3). We note that there is no trend in the relative lengths of the M–X_{ax} and M–X_{eq} bonds, with equal numbers of structures exhibiting longer axial or longer equatorial distances, notwithstanding the shorter M–N distances to the central as opposed to the terminal pyridine rings of the tpy donor.

4. Mononuclear $[\text{M}(\text{tpy})\text{X}_3]$, CN = 6

Of the 33 mononuclear structures in the CSD (see Section 3) containing an $\{\text{M}(\text{tpy})\text{X}_3\}$ motif, 30 exhibit a CN of 6 and, with one exception, are octahedral. The CSD entry with refcode SORSAT, $[\text{Sb}(\text{tpy})\text{F}_3]$, possesses a pseudo-pentagonal bipyramidal structure in which one axial site is occupied by a stereochemically active lone pair of the Sb atom [23]. Of the remaining 29 octahedral $[\text{M}(\text{tpy})\text{X}_3]$ or $[\text{M}(\text{tpy})\text{X}_3]^+$ complexes, 17 are isostructural. These CSD entries are given in Table S1 in the Supplementary Materials, and we note that this family consists only of chlorido and bromido complexes. No coordinates are available for the entries with refcodes QQQCBD $[\text{Al}(\text{tpy})\text{Cl}_3]$ [24], TPYGAC $[\text{Ga}(\text{tpy})\text{Cl}_3]$ [25], TERPIN [26], and TERPTL [26]. However, the space groups and cell dimensions (Table S1) confirm the structural relationship of these compounds to the others in Table S1. For refcodes TPYGAC and TERPIN, coordinates are available for redetermined structures (TPYGAC01, TERPIN01, and TERPIN02). Compounds in this isostructural group for which atomic coordinates are available are given in Table 1. We have omitted the redetermination of the structure of $[\text{Fe}(\text{tpy})\text{Cl}_3]$ at 296 K (refcode HUKIG01) from detailed discussion because of large esds in the metrics [27].

Table 1. Structural data for isostructural octahedral $[M(\text{tpy})\text{X}_3]$ compounds, $\text{X} = \text{Cl}$ or Br .

| Refcode Space Group | M | X | Centroid...Centroid Distance for tpy-tpy π -Stacking within Chain/ \AA ^a (Inter-Ring Plane Angle/ $^\circ$) ^a | Centroid...Centroid Distance for Inter-Chain Close tpy...tpy contacts/ \AA ^b (Interplane Angle/ $^\circ$) ^b | C-H3/3'...Xe _q ; C3/3'...Xe _q / \AA | \angle C- H3/3'...Xe _q / $^\circ$ | Ref. |
|------------------------|----|----|--|---|---|---|------|
| TPYGAC01 $P2_1/n$ | Ga | Cl | 3.84 (5.7) | 4.55 (5.7) | 2.533, 2.677; 3.621(2), 3.756(2) | 178.4, 170.7 | [28] |
| TERPIN01 $P2_1/n$ | In | Cl | 3.79 (5.8) | 4.85 (5.8) | 2.550, 2.575; 3.634 (3), 3.664(2) | 177.3, 173.5 | [29] |
| TERPIN02 $P2_1/n$ | In | Cl | 3.83 (5.8) | 4.92 (5.8) | 2.592, 2.607; 3.676(4), 3.696(3) | 177.8, 173.6 | [30] |
| KEZZOH $P2_1/n$ | Sc | Cl | 3.82 (6.3) | 4.88 (6.3) | 2.547, 2.573; 3.635(6), 3.658(7) | 176.5, 173.5 | [31] |
| PAXVAM $P2_1/n$ | Mn | Cl | 3.79 (5.5) | 4.79 (5.5) | 2.583, 2.602; 3.671(3), 3.689(3) | 177.3, 176.7 | [32] |
| HUJKIG $P2_1/n$ | Fe | Cl | 3.79 (5.6) | 4.61 (5.6) | 2.525, 2.608; 3.613(2), 3.689(2) | 178.0, 171.5 | [33] |
| HUJKIG02 $P2_1/n$ | Fe | Cl | 3.80 (5.7) | 4.62 (5.7) | 2.535, 2.618; 3.623(2), 3.699(2) | 178.3, 171.6 | [34] |
| CUBQEV $P2_1/n$ | Ru | Cl | 3.94 (6.8) | 4.59 (6.8) | 2.58, 2.90; 3.67(1), 3.96(1) | 173.0, 166.1 | [35] |
| BONRAY $P2_1/n$ | Ir | Cl | 3.90 (6.5) | 4.49 (6.5) | 2.434, 2.692; 3.522(4), 3.771(4) | 177.0, 170.5 | [36] |
| WOLDOQ $P2_1/n$ | Os | Cl | 3.88 (6.7) | 4.60 (6.7) | 2.468, 2.699; 3.538(4), 3.780(4) | 171.7, 167.2 | [37] |
| LOBXAD $P2_1/n$ | Ga | Br | 3.93 (5.7) | 4.60 (5.7) | 2.653, 2.806; 3.740(3), 3.892(3) | 176.4, 174.6 | [28] |
| RARVIT $P2_1/n$ | Cr | Br | 3.99 (6.7) | 4.65 (6.7) | 2.594, 2.828; 3.680(3), 3.913(3) | 174.6, 174.2 | [38] |
| BONREC $P2_1/n$ | Ir | Br | 4.01 (7.5) | 4.59 (7.5) | 2.537, 2.867; 3.62(2), 3.95(2) | 175.8, 173.8 | [36] |

^a As defined in Figures 1 and 2. ^b Close tpy...tpy contacts between red and blue chains as defined in Figure 2c.

Figure 1 illustrates the packing of molecules in the solid-state structure of $[\text{Fe}(\text{tpy})\text{Cl}_3]$ (refcode HUJKIG [33]), which is representative of the compounds listed in Table 1. The original reports of these structures gave little description of the crystal packing. Reid and coworkers described the packing in $[\text{Sc}(\text{tpy})\text{Cl}_3]$ (refcode KEZZOH) in terms of " π -stacking interactions (3.82 \AA) between the aromatic ring of the terpy ligand of the adjacent molecule, connecting them into 1D zig-zag chains" [31]. This interaction can be identified in the chains that follow the crystallographic b -axis with the cited value of 3.82 \AA referring to the centroid...centroid distance (Figures 1a and 2a). The diagram in Figure 2b illustrates how these π -stacking interactions relate to the packing as viewed down the b -axis (compare Figure 2b with 1b). The centroid...centroid distance of 3.82 \AA is typical for π -interactions between pairs of coordinated pyridine ligands [8]. Centroid...centroid distances and interring plane angles corresponding to those shown for $[\text{Sc}(\text{tpy})\text{Cl}_3]$ in Figure 2 were measured using Mercury [16] for all the compounds in Table 1. The centroid...centroid distances range from 3.79 to 4.01 \AA (Table 1, column 4), with the longest distances observed in the bromido derivatives. Figure 2c illustrates the packing of adjacent chains along the crystallographic a -axis. Although the chains lie parallel to one another, the slippage of the tpy units between

red and blue chains in Figure 2c results in there being significantly weaker face-to-face π -interactions between these chains. This is quantified in the metrics presented in Table 1 (column 5) for the inter-chain close contacts between tpy domains.

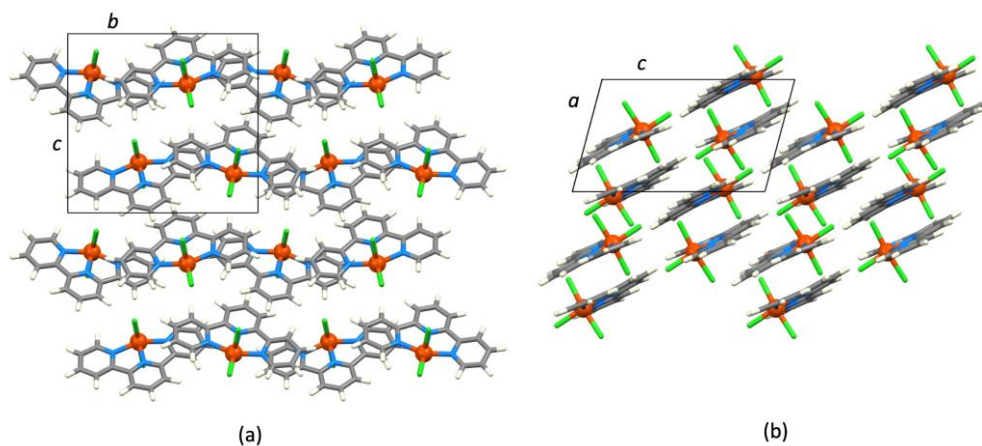


Figure 1. Packing of molecules in $[\text{Fe}(\text{tpy})\text{Cl}_3]$ (CSD refcode HUKJIG [33]). Views down the (a) crystallographic a -axis, and (b) crystallographic b -axis.

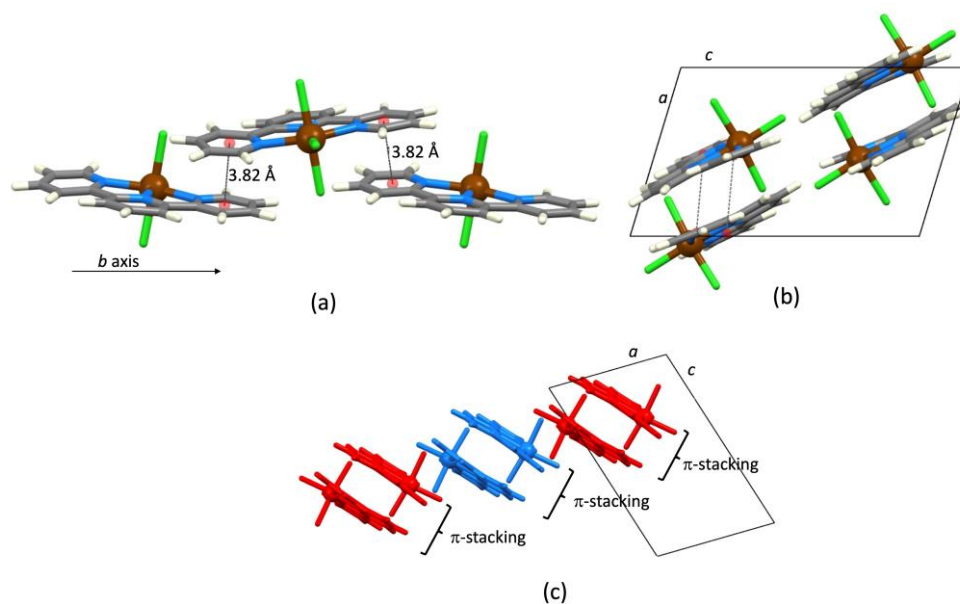


Figure 2. (a) Arrangement of $[\text{Sc}(\text{tpy})\text{Cl}_3]$ molecules into chains through π -stacking as described by Reid and coworkers, and (b) a view down the b -axis showing the same π -stacking in part (a) for comparison with Figure 1b (refcode KEZZOH) [31]. (c) Arrangement of adjacent chains (blue and red) containing the π -stacking defined in diagrams (a,b). Note that in the discussion, the term “chain” refers to the π -stacked chains defined in this figure.

We now turn our attention to the role that C–H...X interactions play in the compounds presented in Table 1. The presence of “extensive intermolecular hydrogen bonding” in the crystal packing of $[\text{Ru}(\text{tpy})\text{Cl}_3]$ (refcode CUBQEV [35]) and $[\text{In}(\text{tpy})\text{Cl}_3]$ (refcode TERPIN01 [29]) was noted by the original authors. However, the metrics of these CH...X contacts have not, to our knowledge, been discussed, and there have been no comparisons made across the series of isostructural complexes in Table 1. If we return to the crystal packing in $[\text{Fe}(\text{tpy})\text{Cl}_3]$ (Figure 1) and focus on C–H...Cl close contacts, we observe that the equatorial Cl atom (Cl_{eq} , defined in Scheme 3) forms a bifurcated contact with atoms H3 and H3' of an adjacent molecule (Figure 3a and Table 1) allowing the crystal packing to be

described in terms of chains supported by non-classical C–H3/H3'...Cl_{eq} hydrogen bonds. Corresponding C–H3/H3'...X_{eq} contacts for all compounds in this octahedral [M(tpy)X₃] family are given in Table 1 and exhibit similar metrics. A comparison of Figure 3a with Figure 1a shows that the hydrogen-bonded chains are orthogonal to the chains defined by the tpy...tpy π -stacking interactions.

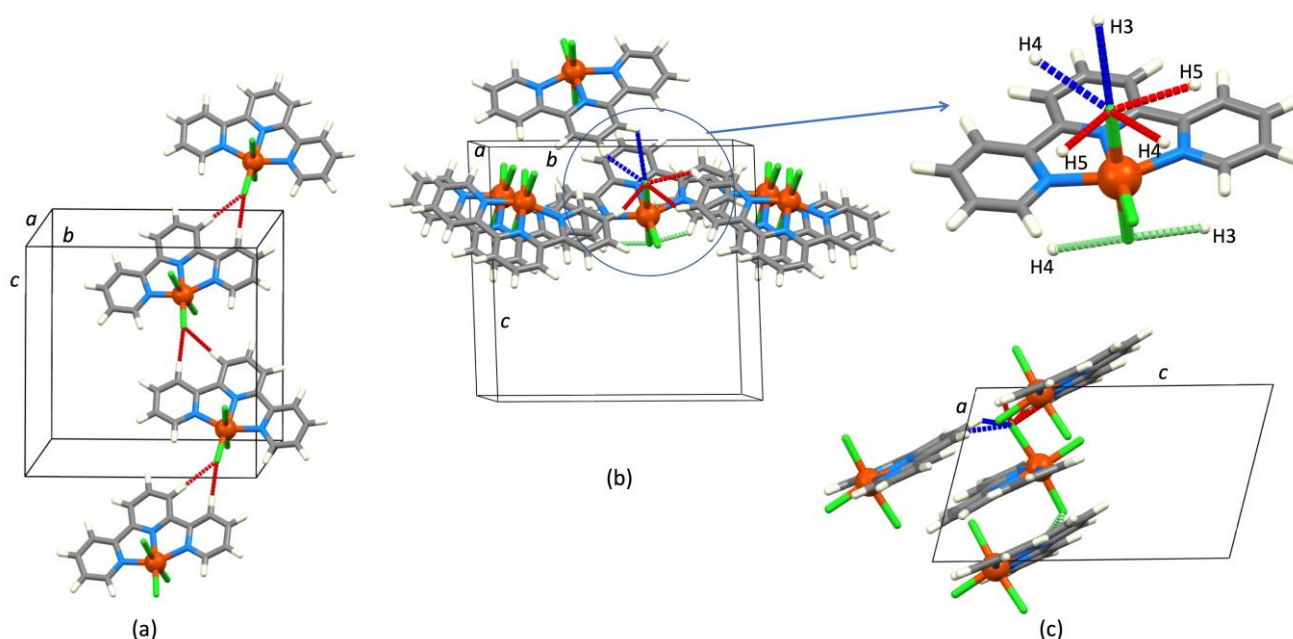


Figure 3. C–H...Cl packing interactions in [Fe(tpy)Cl₃] (refcode HUKJIG [33]). (a) Bifurcated Cl_{eq}...H3/H3' contacts (shown in red). (b,c) Cl_{ax}...H3/H4/H5 interactions: those within a chain (as defined in Figure 2c) are shown in pale green, those between chains (as defined in Figure 2c) are in red, and those to the next set of chains are shown in blue.

Further analysis of the structure of [Fe(tpy)Cl₃] (Figure 3) shows that the axial Cl atoms (Cl_{ax}) are involved in intermolecular C–H3/H4/H5...Cl_{ax} interactions within and between π -stacked chains (the latter defined as in Figure 2c). These contacts are depicted by the pale-green and red hashed lines in Figure 3b,c, respectively. There are additional C–H3/H4...Cl_{ax} contacts (shown in blue in Figure 3b,c) to the adjacent set of chains, and this interaction is also supported by a face-to-face π -stacking contact between the central pyridine rings of two tpy ligands (centroid...centroid = 3.98 Å). The metrics for the C–H3/H4/H5...Cl_{ax} interactions are given in Table S2 (see Supplementary Materials) for all the [M(tpy)X₃] compounds.

We move now from the 17 isostructural [M(tpy)X₃] compounds to the 12 octahedral coordination entities, which crystallize either with lattice solvent or are charged. The addition of water molecules to the crystal structure provides additional hydrogen-bond sites, and the combination of fluorido ligands and lattice water leads to strong F...H–OH hydrogen bonds as a dominant packing motif in [Al(tpy)F₃]·3H₂O (refcode NUHBOJ [39]), [Ga(tpy)F₃]·3H₂O (refcode NUHCOK [39]), [Fe(tpy)F₃]·3H₂O (refcode JOC-TIH [40]), [Cr(tpy)F₃]·2.5H₂O (refcode VAFDIR [19]), and [Mn(tpy)F₃]·MeOH·0.33H₂O (refcode ALIYOJ [41]). These complement the face-to-face π -stacking of tpy domains.

The compounds [Cr(tpy)Cl₃]·DMSO (refcode LEWKEE [42]) and [Rh(tpy)Cl₃]·DMSO (refcode IGAWIW [43]) are isostructural and exhibit a centrosymmetric dinuclear motif supported by C–H3/H3'...Cl_{ax} hydrogen bonds (Figure 4a) and a face-to-face tpy...tpy π -interaction (Figure 4b). Metrics for the interaction are given in Table 2. The motif in Figure 4 is reminiscent of those present in [M(bpy)₂X₂] compounds [13] and allows us to draw a parallel between the role of the bpy H3/H3' and tpy H3/H3' atoms in crystal packing.

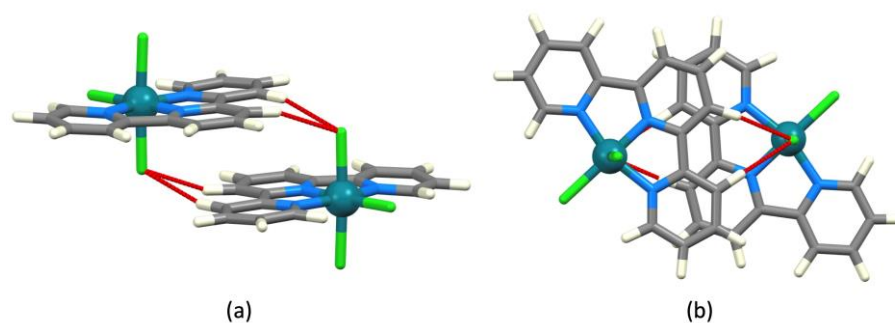


Figure 4. Dimeric packing motif in $[\text{Rh}(\text{tpy})\text{Cl}_3]\cdot\text{DMSO}$ (refcode IGAWIW [43]) showing (a) C–H3/H3'...Cl_{ax} contacts and (b) tpy...tpy offset π -stacking.

Table 2. Metric parameters for the face-to-face π -stacking and C–H3/H3'...X_{ax} contacts in the centrosymmetric dimeric motifs in $[\text{M}(\text{tpy})\text{Cl}_3]\cdot\text{DMSO}$ (M = Cr, Rh).

| Refcode Space Group | M | Centroid...Centroid/Å | C–H...X; C...X/Å | $\angle\text{C–H...X}^\circ$ | C–H...X; C...X/Å | $\angle\text{C–H...X}^\circ$ | Ref. |
|------------------------|----|-----------------------|---------------------|------------------------------|---------------------|------------------------------|------|
| LEWKEE $P\bar{1}$ | Cr | 3.81 | 2.622; 3.644(3) | 156.0 | 2.629; 3.635(2) | 153.3 | [42] |
| IGAWIW $P\bar{1}$ | Rh | 3.81 | 2.595; 3.638(6) | 160.3 | 2.615; 3.663(7) | 161.2 | [43] |

The platinum(IV) compounds $[\text{Pt}(\text{tpy})\text{X}_3][\text{PF}_6]$ (X = Cl, Br), $[\text{Pt}(\text{tpy})\text{Br}_3]\text{Br}$ and $[\text{Pt}(\text{tpy})\text{Br}_3][\text{Br}_3]$ (refcodes YOZNUZ, YOZNEJ, YOZNOT, and YOZNIN [44]) form the last group of compounds containing a mononuclear, octahedral $[\text{M}(\text{tpy})\text{X}_3]$ unit. Taylor et al. report that there are “no unusually short intermolecular contacts”, with the exception of a short $\text{Br}_{\text{ax}}\cdots\text{Br}^-$ contact in $[\text{Pt}(\text{tpy})\text{Br}_3]\text{Br}$ [44]. We note that in $[\text{Pt}(\text{tpy})\text{Br}_3]\text{Br}$, the H3/H3', H5', and H4'' atoms form hydrogen bonds to bromide ions (Figure 5a), with C–H...Br and C...Br distances in the range 2.613–2.909 Å, and 3.619(5)–3.719(5) Å, respectively, and $\angle\text{C–H...Br}$ in the range 125.2–165.3°. There are additional weak C–H...Br_{ax} and C–H...Br_{eq} interactions. The view of the packing motif in Figure 5b illustrates that tpy ligands in adjacent molecules are not involved in efficient π -stacking (the centroid...centroid distance between the two central pyridine rings = 4.39 Å). The dominance of packing interactions involving hydrogen bonds to Br^- is consistent with the bromide ion being a stronger hydrogen-bond acceptor than a metal-bound Br atom.

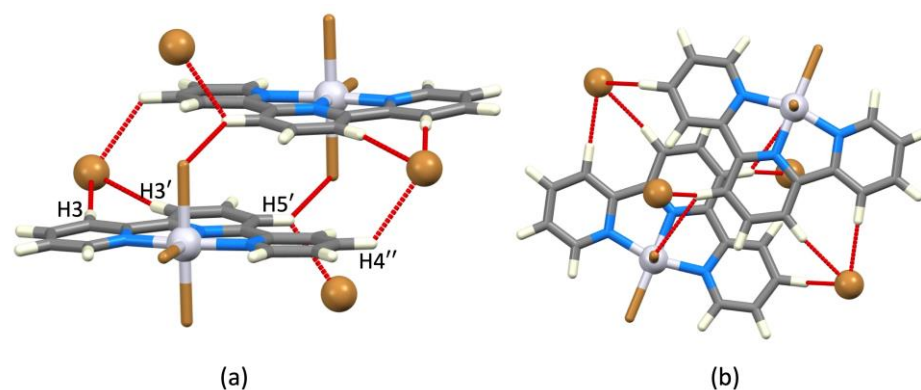


Figure 5. (a) C–H3/H3'/H5'/H4''...Br[−] and C–H5'...Br_{ax} hydrogen bonds in $[\text{Pt}(\text{tpy})\text{Br}_3]\text{Br}$ (refcode YOZNOT [44]); (b) the same motif as in (a) viewed from above to illustrate the absence of efficient π -stacking.

5. Mononuclear $[M(\text{tpy})X_3(\text{Y})]$, ($\text{Y} = \text{X}, \text{OH}_2, \text{MeOH}$), $\text{CN} = 7$

The search of the CSD for the $\{M(\text{tpy})X_3\}$ moiety revealed three entries with mononuclear, 7-coordinate structures (refcodes AVOJIH, KEZZUN, and KIBBUV). Each introduces a new hydrogen-bond acceptor in the form of coordinated H_2O or MeOH in $[M(\text{tpy})\text{Cl}_3(\text{OH}_2)]$ ($M = \text{Y}, \text{Lu}$) [31] and $[\text{Bi}(\text{tpy})\text{Br}_3(\text{MeOH})]$ [45]. Pentagonal bipyramidal $[\text{Y}(\text{tpy})\text{Cl}_3(\text{OH}_2)]$ and $[\text{Lu}(\text{tpy})\text{Cl}_3(\text{OH}_2)]$ are isostructural, and Reid and coworkers [31] comment on the $\text{Cl}\dots\text{HOH}$ hydrogen bonding between adjacent molecules. We note the additional presence of bifurcated $\text{Cl}\dots\text{H3}/\text{H3}'$ interactions leading to the assembly of chains, as shown in Figure 6. Metrics for the interactions are given in Table 3. The crystal packing in $[\text{Bi}(\text{tpy})\text{Br}_3(\text{MeOH})]$ was described by Knope and coworkers in terms of intermolecular $\text{tpy}\dots\text{tpy}$ π -stacking and $\text{O}\text{--}\text{H}\dots\text{Br}$ interactions [45]. However, we again note the presence of bifurcated $\text{Br}\dots\text{H3}/\text{H3}'$ contacts for both crystallographically independent molecules. The $\text{C}\text{--}\text{H}\dots\text{Br}$ distances are in the range 2.713–3.042 Å, with $\text{C}\dots\text{Br}$ distances of 3.627(4)–3.966(4) Å and $\text{C}\text{--}\text{H}\dots\text{Br}$ angles in the range 151.7–177.3°.

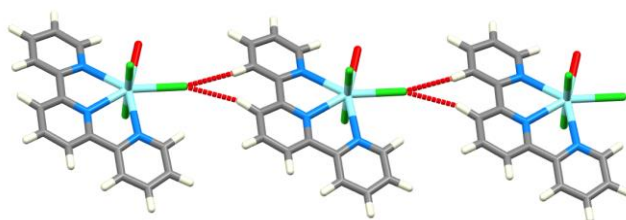


Figure 6. Part of one hydrogen-bonded chain involving $\text{C}\text{--}\text{H3}/\text{H3}'\dots\text{Cl}$ interactions in $[\text{Y}(\text{tpy})\text{Cl}_3(\text{OH}_2)]$ (refcode KEZZUN [31]).

Table 3. Metric parameters for the $\text{C}\text{--}\text{H3}/\text{H3}'\dots\text{Cl}_{\text{eq}}$ contacts in $[M(\text{tpy})\text{Cl}_3(\text{OH}_2)]$ ($M = \text{Y}, \text{Lu}$).

| Refcode Space Group | M | $\text{C}\text{--}\text{H}\dots\text{Cl}; \text{C}\dots\text{Cl}/\text{Å}$ | $\angle\text{C}\text{--}\text{H}\dots\text{Cl}/^\circ$ | $\text{C}\text{--}\text{H}\dots\text{Cl}; \text{C}\dots\text{Cl}/\text{Å}$ | $\angle\text{C}\text{--}\text{H}\dots\text{Cl}/^\circ$ | Ref. |
|------------------------|----|--|--|--|--|------|
| KEZZUN $P\bar{1}$ | Y | 2.634; 3.700(5) | 166.2 | 2.831; 3.862(6) | 157.9 | [31] |
| KIBBUV $P\bar{1}$ | Lu | 2.638; 3.706(3) | 166.7 | 2.773; 3.825(4) | 162.3 | [31] |

6. Dinuclear $[M_2(\text{tpy})_2X_n(\mu\text{--}X)_2]$ ($n = 2, 4$), $[M_2(\text{tpy})_2X_2(\text{OH}_2)_2(\mu\text{--}X)_2]$, $[M_2(\text{tpy})_2X_4(\text{OH}_2)_2(\mu\text{--}X)_2]$ and $[M_2(\text{tpy})_2X_2(\text{DMF})_2(\mu\text{--}\text{Cl})_2]$ (DMF = dimethylformamide)

As detailed in Section 3, the search of the CSD gave 11 hits for dinuclear species containing the $\{M(\text{tpy})X_3\}$ motif. In only two of these does the metal atom have $\text{CN} = 6$. In $[\text{Pb}_2(\text{tpy})_2\text{I}_2(\mu\text{--}\text{I})_2]$ (refcode RAQQOP), packing is dominated by $\text{tpy}\dots\text{tpy}$ π -stacking, as reported by Engelhardt et al. [20]. Reid and coworkers point to the “extensive hydrogen bonding linking the lattice water molecules, the cations and the $[\text{PF}_6]^-$ anions” in $[\text{Ga}_2(\text{tpy})_2\text{F}_2(\mu\text{--}\text{F})_2][\text{PF}_6]_2\cdot 4\text{H}_2\text{O}$ (refcode NUHBIP) [39]. However, it is pertinent to our investigation to note the role of the tpy H3 and H3' atoms in $\text{C}\text{--}\text{H}\dots\text{O}$ and $\text{C}\text{--}\text{H}\dots\text{F}$ hydrogen bonds in $[\text{Ga}_2(\text{tpy})_2\text{F}_2(\mu\text{--}\text{F})_2][\text{PF}_6]_2\cdot 4\text{H}_2\text{O}$ (Figure 7a). Metrics for the interactions are given in the caption of Figure 7a. The remaining dinuclear complexes all contain chlorido ligands and feature large *s*-, *p*- or *f*-block metal centers with $\text{CN} = 7$ or 8. Four compounds of stoichiometry $[M_2(\text{tpy})_2\text{Cl}_4(\text{OH}_2)_2(\mu\text{--}\text{Cl})_2]$ with $M = \text{La}, \text{Nd}, \text{Sm}, \text{Eu}$ ($\text{CN} = 8$) are isostructural (refcodes KIBBOP, EXIDIE, YECRUT and EXODOL [17,31,46]) and the packing between the centrosymmetric dimers has been described by Loiseau and coworkers in terms of π -stacking of tpy domains [17]. The structure of $[\text{Eu}_2(\text{tpy})_2\text{Cl}_4(\text{OH}_2)_2(\mu\text{--}\text{Cl})_2]$ shown in Figure 7b is representative of this group of compounds. The H3/H3' and H5'/H3'' pairs of atoms of each tpy ligand are involved in bifurcated $\text{Cl}\dots\text{H}/\text{H}$ interactions, the Cl atom being either a terminal or bridging chlorido ligand of an adjacent molecule. The metric parameters for the interactions are given in Table 4 and typify the short contacts that

are observed for similar interactions described above. An analogous motif is found in $[\text{Ca}_2(\text{tpy})_2\text{Cl}_2(\text{DMF})_2(\mu\text{-Cl})_2]$ (Table 4, refcode TAQSEJ [47]) and $[\text{Bi}_2(\text{tpy})_2\text{Cl}_4(\mu\text{-Cl})_2]\cdot\text{H}_2\text{O}$ (distorted pentagonal bipyramidal Bi, refcode AVOVEP [45]). The bismuth compound has two crystallographically independent molecules, one of which forms four intermolecular, bifurcated hydrogen bonds between tpy atoms H3/H3' or H5'/H3'' and the axial Cl atoms of adjacent molecules (Table 4). Interestingly, although there is intermolecular tpy...tpy π -stacking in $[\text{Bi}_2(\text{tpy})_2\text{Cl}_4(\mu\text{-Cl})_2]\cdot\text{H}_2\text{O}$ [45], there are no comparable interactions in anhydrous $[\text{Bi}_2(\text{tpy})_2\text{Cl}_4(\mu\text{-Cl})_2]$ (refcode QURDUF), as noted by the original authors [48]. Crystal packing in the latter is dominated by C–H...Cl hydrogen bonds, including a bifurcated contact involving tpy H atoms H3/H3' (Table 4). Crystal packing in $[\text{Pb}_2(\text{tpy})_2\text{Cl}_2(\text{OH}_2)_2(\mu\text{-Cl})_2]$ (CN = 7, refcode RAQQEF [20]) involves face-to-face tpy...tpy π -stacking (Figure 8a, centroid...centroid = 3.76 Å) combined with C–H...Cl and C–H...O contacts. Although the tpy H3, H4, H5, H3', H5', and H5'' atoms are all close to Cl atoms of adjacent molecules in the crystal structure, the shortest contacts are those involving H3 and H3' (Table 4). A comparison of Figure 8a with Figure 4b reveals a common packing motif in $[\text{Pb}_2(\text{tpy})_2\text{Cl}_2(\text{OH}_2)_2(\mu\text{-Cl})_2]$, $[\text{Cr}(\text{tpy})\text{Cl}_3]\cdot\text{DMSO}$ and $[\text{Rh}(\text{tpy})\text{Cl}_3]\cdot\text{DMSO}$, i.e., a centrosymmetric unit supported by C–H3/H3'...Cl_{terminal} hydrogen bonds and a face-to-face tpy...tpy π -interaction. This is reminiscent of the pervasive packing motif observed in *cis*- $[\text{M}(\text{bpy})_2\text{X}_2]$ compounds [13]. In the case of $[\text{Pb}_2(\text{tpy})_2\text{Cl}_2(\text{OH}_2)_2(\mu\text{-Cl})_2]$, the presence of the second tpy ligand leads to the formation of hydrogen-bonded 1D-chains (Figure 8b).

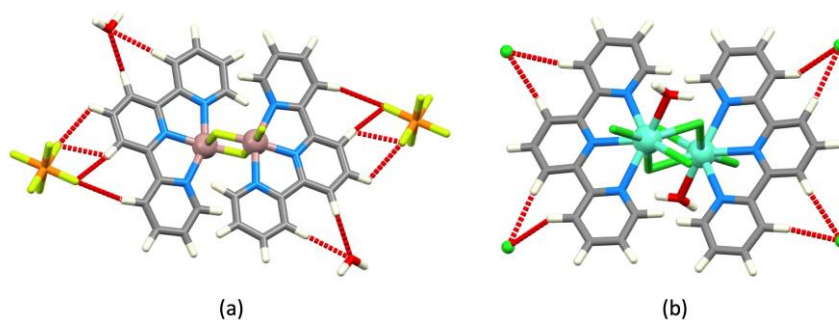


Figure 7. (a) C–H...F and C–H...O hydrogen bonds in $[\text{Ga}_2(\text{tpy})_2\text{F}_2(\mu\text{-F})_2][\text{PF}_6]_2\cdot 4\text{H}_2\text{O}$ (refcode NUH-BIP [39]). Metrics: C–H...O = 2.419, 2.485 Å; C...O = 3.508(5), 3.558(3) Å, $\angle\text{C–H...O} = 178.9, 168.1^\circ$. C–H3/H3'...F = 2.302, 2.721, 2.397 Å; C...F = 3.386(4), 3.789(6), 3.045(5) Å, $\angle\text{C–H3/H3'...F} = 173.2, 166.9, 116.6^\circ$; C–H4'...F = 2.474 Å; C...F = 3.092(4) Å, $\angle\text{C–H4'...F} = 114.7^\circ$. (b) C–H3/H3'...Cl and C–H5'/H3''...Cl contacts in the centrosymmetric dimer $[\text{Eu}_2\text{Cl}_4(\text{OH}_2)_2(\mu\text{-Cl})_2]$ (refcode EX-ODOL [17]); see text and Table 4.

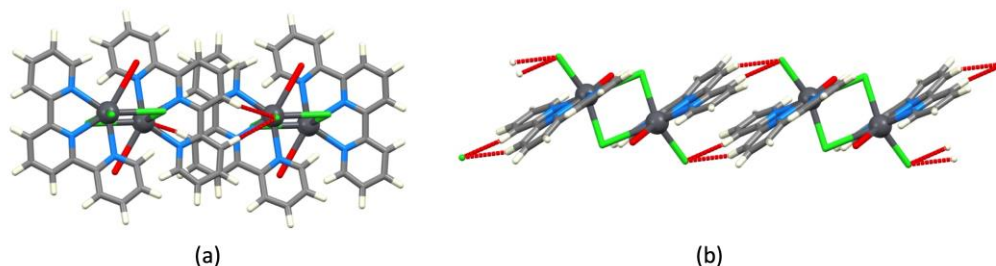


Figure 8. (a) Packing interactions in $[\text{Pb}_2(\text{tpy})_2\text{Cl}_2(\text{OH}_2)_2(\mu\text{-Cl})_2]$ (refcode RAQQEF [20]) are dominated by π -stacking between tpy ligands, and hydrogen bonds between terminal Cl and tpy H3/H3' atoms. (b) The C–H3/H3'...Cl contacts lead to a hydrogen-bonded chain.

Table 4. Metric parameters for the bifurcated C–H3/H3'...Cl and C–H5'/H3''...Cl contacts in [M₂Cl₄(OH₂)₂(μ-Cl)₂] (M = La, Nd, Sm, Eu) and [Bi₂(tpy)₂Cl₄(μ-Cl)₂]·H₂O.

| Refcode Space Group | M | C–H3/H3'...Cl; C...Cl/Å | ∠C– H3/H3'...Cl/° | C–H5'/H3''...Cl; C...Cl/Å | ∠C– H5'/H3''...Cl/° | Ref. |
|--|----|-------------------------------------|----------------------|-------------------------------------|------------------------|------|
| KIBBOP <i>P</i> $\bar{1}$ | La | 2.734, 2.798; 3.530(3), 3.743(4) | 141.8, 173.0 | 2.792, 2.652; 3.713(3), 3.592(3) | 163.4, 170.1 | [31] |
| EXODIF <i>P</i> $\bar{1}$ | Nd | 2.93, 2.85; 3.554(2), 3.791(3) | 125, 171 | 2.75, 2.70; 3.741(2), 3.621(2) | 161, 168 | [17] |
| YECRUT <i>P</i> $\bar{1}$ | Sm | 2.70, 2.96; 3.551(4), 3.802(4) | 146, 170 | 2.83, 2.84; 3.737(4), 3.622(4) | 159, 165 | [46] |
| EXODOL <i>P</i> $\bar{1}$ | Eu | 2.661, 2.724; 3.568(3), 3.797(4) | 140.3, 168.6 | 2.678, 2.550; 3.726(3), 3.627(2) | 161.3, 170.0 | [17] |
| TAQSEJ <i>C</i> 2/ <i>c</i> | Ca | 2.524, 2.682; 3.61(1), 3.76(1) | 171.8, 169.9 | 2.675, 2.776; 3.75(3), 3.83(2) | 170.4, 163.0 | [47] |
| AVOVEP <i>P</i> $\bar{1}$ | Bi | 2.539, 2.781; 3.564(7), 3.862(7) | 156.4, 171.7 | 2.657, 2.652; 3.723(7), 3.722(8) | 166.2, 167.3 | [45] |
| QURDUF <i>P</i> 2 ₁ / <i>n</i> | Bi | 2.556, 2.643; 3.626(4), 3.706(4) | 167.5, 164.9 | | | [48] |
| RAQQEF <i>P</i> $\bar{1}$ | Pb | 2.658, 2.695; 3.668(7), 3.773(8) | 153.9, 170.7 | | | [20] |

In the remaining dinuclear complex(refcode AVOVIT [45]), an additional chelating ligand is present, and we have chosen to exclude this compound from the detailed discussion.

7. Conclusions

We have carried out a search of the CSD [10] for compounds containing [M(tpy)X₃] motifs (M = any metal; X = any halogen). After discarding seven compounds(see Section 3), 44 solid-state structures remained, 33 mononuclear compounds (CN = 6 or 7) and 11 dinuclear species (CN = 6, 7, or 8).

Seventeen mononuclear [M(tpy)X₃] compounds (M = group 13 metal or a first, second, or third-row d-block metal, and X = Cl or Br) crystallize without lattice solvent. These octahedral [M(tpy)X₃] compounds are isostructural, despite the increase in the size of (i) the metal atom on descending a periodic group or (ii) on going from Cl to Br with the associated lengthening of the M–X bonds. Earlier descriptions of the crystal packing in individual [M(tpy)X₃] compounds focused on either tpy...tpy π -stacking or C–H...X interactions. The overview presented here demonstrates that face-to-face π -stacking of pyridine rings and C–H3/H3'...X hydrogen bonding are synergic. Regardless of coordination number and compound nuclearity, a recurring packing feature of the remaining compounds is the presence of bifurcated Cl...H3/H3' interactions, complemented in some cases by Cl...H5'/H3'' interactions. This is consistent with the acidic nature of the H3, H3', H5', and H3'' atoms of a coordinated tpy ligand [14]. The results complement the work of Brammer, Orpen, and coworkers, who have analyzed hydrogen bond formation by metal-bound chlorido ligands [49].

We note that the five octahedral [M(tpy)F₃] complexes in the CSD crystallize as hydrates with strong F...H–OH hydrogen bonding dominating the crystal packing.

Supplementary Materials: The following supporting information can be downloaded at: <https://www.mdpi.com/article/10.3390/cryst13060885/s1>, Table S1. Crystallographic cell dimensions for the compounds in Table 1; Table S2. C–H3/H4/H5...Cl_{ax} interactions in [M(tpy)X₃], X = Cl or Br (see Figure 3b).

Author Contributions: The authors contributed equally to the writing of this work. Conceptualization: E.C.C. Data mining and evaluation: E.C.C. and C.E.H. All authors have read and agreed to the published version of the manuscript.

Funding: This research received no external funding.

Data Availability Statement: Not applicable.

Acknowledgments: We thank the University of Basel for its support.

Conflicts of Interest: The authors declare no conflict of interest.

References

1. Constable, E.C. The Coordination Chemistry of 2,2':6',2''-Terpyridine and Higher Oligopyridines. *Adv. Inorg. Chem.* **1986**, *30*, 69–121. [[CrossRef](#)]
2. Schubert, U.S.; Hofmeier, H.; Newkome, G.R. *Modern Terpyridine Chemistry*; Wiley-VCH Verlag & Co.: Weinheim, Germany, 2006.
3. Constable, E.C. 2,2':6',2''-Terpyridines: From chemical obscurity to common supramolecular motifs. *Chem. Soc. Rev.* **2007**, *36*, 246–253. [[CrossRef](#)] [[PubMed](#)]
4. Wei, C.; He, Y.; Shi, X.; Song, Z. Terpyridine-metal complexes: Applications in catalysis and supramolecular chemistry. *Coord. Chem. Rev.* **2019**, *385*, 1–19. [[CrossRef](#)] [[PubMed](#)]
5. McMurtie, J.; Dance, I. Crystal packing in metal complexes of 4'-phenylterpyridine and related ligands: Occurrence of the 2D and 1D terpy embrace arrays. *CrystEngComm* **2009**, *11*, 1141–1149. [[CrossRef](#)]
6. McMurtie, J.; Dance, I. Alternative metal grid structures formed by $[M(\text{terpy})_2]^{2+}$ and $[M(\text{terpyOH})_2]^{2+}$ complexes with small and large tetrahedral dianions, and by $[\text{Ru}(\text{terpy})_2]^0$. *CrystEngComm* **2010**, *12*, 2700–2710. [[CrossRef](#)]
7. McMurtie, J.; Dance, I. Alternative two-dimensional embrace nets formed by metal complexes of 4'-phenylterpyridine crystallised with hydrophilic anions. *CrystEngComm* **2010**, *12*, 3207–3217. [[CrossRef](#)]
8. Janiak, C. A critical account on π - π stacking in metal complexes with aromatic nitrogen-containing ligands. *J. Chem. Soc. Dalton Trans.* **2000**, *21*, 3885–3896. [[CrossRef](#)]
9. Dance, I.; Scudder, M. Molecular embracing in crystals. *CrystEngComm* **2009**, *11*, 2233–2247. [[CrossRef](#)]
10. Groom, C.R.; Bruno, I.J.; Lightfoot, M.P.; Ward, S.C. The Cambridge Structural Database. *Acta Crystallogr. Sect. B* **2016**, *72*, 171–179. [[CrossRef](#)]
11. Constable, E.C.; Housecroft, C.E. Halide Ion Embraces in Tris(2,2'-bipyridine)metal Complexes. *Crystals* **2020**, *10*, 671. [[CrossRef](#)]
12. Constable, E.C.; Housecroft, C.E. Embracing $[\text{XY}_3]^{m-}$ and $[\text{XY}_4]^{m-}$ anions in salts of $[\text{M}(\text{bpy})_3]^{q+}$. *Crystals* **2023**, *13*, 97. [[CrossRef](#)]
13. Constable, E.C.; Housecroft, C.E. Packing motifs in $[\text{M}(\text{bpy})_2\text{X}_2]$ coordination compounds (bpy = 2,2'-bipyridine; X = F, Cl, Br, I). *Crystals* **2023**, *13*, 505. [[CrossRef](#)]
14. Constable, E.C.; Seddon, K.R. A Deuterium Exchange Reaction of the Tris-(2,2'-bipyridine)ruthenium(II) Cation: Evidence for the Acidity of the 3,3'-Protons. *J. Chem. Soc. Chem. Commun.* **1982**, *1*, 34–36. [[CrossRef](#)]
15. Bruno, I.J.; Cole, J.C.; Edgington, P.R.; Kessler, M.; Macrae, C.F.; McCabe, P.; Pearson, J.; Taylor, R. New software for searching the Cambridge Structural Database and visualising crystal structures. *Acta Crystallogr. Sect. B* **2002**, *58*, 389–397. [[CrossRef](#)] [[PubMed](#)]
16. Macrae, C.F.; Sovago, I.; Cottrell, S.J.; Galek, P.T.A.; McCabe, P.; Pidcock, E.; Platings, M.; Shields, G.P.; Stevens, J.S.; Towler, M.; et al. Mercury 4.0: From visualization to analysis, design and prediction. *J. Appl. Cryst.* **2020**, *53*, 226–235. [[CrossRef](#)]
17. Lhoste, J.; Perez-Campos, A.; Henry, N.; Loiseau, T.; Rabu, P.; Abraham, F. Chain-like and dinuclear coordination polymers in lanthanide (Nd, Eu)oxochloride complexes with 2,2':6',2''-terpyridine: Synthesis, XRD structure and magnetic properties. *Dalton Trans.* **2011**, *40*, 9136–9144. [[CrossRef](#)] [[PubMed](#)]
18. Wang, G.-F.; Zhang, X.; Sun, S.-W.; Yao, C.-Z.; Liu, Z.-R.; Wang, Y.-C.; Liu, Y.-Z. Synthesis and structural characterization of a novel copper(II)/lead(II) heterometallic organic-inorganic hybrid. *Z. Naturforsch. B* **2015**, *70*, 617–623. [[CrossRef](#)]
19. Birk, T.; Magnussen, M.J.; Piligkos, S.; Weihe, H.; Holten, A.; Bendix, J. Alkali metal cation complexation and solvent interactions by robust chromium(III) fluoride complexes. *J. Fluor. Chem.* **2010**, *131*, 898–906. [[CrossRef](#)]
20. Engelhardt, L.M.; Harrowfield, J.M.; Miyamae, H.; Patrick, J.M.; Skelton, B.W.; Soudi, A.A.; White, A.H. Lewis-Base Adducts of Lead(II) Compounds. XVII Synthetic and Structural Studies of Some 1:1 Adducts of 2,2':6',2''-Terpyridine with Lead(II) Salts. *Aust. J. Chem.* **1996**, *49*, 1135–1146. [[CrossRef](#)]
21. Tershansy, M.A.; Goforth, A.M.; Smith, M.D.; zur Loye, H.-C. The Synthesis and Crystal Structure of $[\text{BiI}_2(\text{tpy})_2][\text{BiI}_7(\text{tpy})]$: A New Metal Halide Material. *J. Chem. Cryst.* **2008**, *38*, 453–459. [[CrossRef](#)]
22. Lewis, K.M.; Kelley, J.; Petersen, L., Jr.; Smith, M.D.; Severance, R.C.; Vaughn, S.A.; zur Loye, H.-C. Synthesis and Crystal Structure of an Iodobismuthate Incorporating Both a Cationic and Anionic Bi(III) Complex Ion. *J. Chem. Crystallogr.* **2010**, *40*, 867–871. [[CrossRef](#)]
23. Battaglia, L.P.; Corradi, A.B.; Pelosi, G.; Cantoni, A.; Alonzo, G.; Bertazzi, N. Crystal and Molecular Structure of Antimony Trifluoride Terpyridine 1:1 Adduct: A Case of Pseudo-pentagonal-bipyramidal Geometry. *J. Chem. Soc. Dalton Trans.* **1991**, *11*, 3153–3155. [[CrossRef](#)]
24. Beran, G.; Dymock, K.; Patel, H.A.; Carty, A.J.; Boorman, P.M. Solid-State Structures of Group IIIb Metal Chloride Adducts with 2,2',2''-Terpyridyl. *Inorg. Chem.* **1972**, *11*, 896–898. [[CrossRef](#)]

25. Beran, G.; Carty, A.J.; Patel, H.A.; Palenik, G.J. A trans-Effect in Gallium Complexes: The Crystal Structure of Trichloro-(2,2',2''-terpyridyl)gallium(III). *J. Chem. Soc. D Chem. Comm.* **1970**, 222–223. [[CrossRef](#)]
26. Palenik, G.J.; Dymock, K. *American Crystallographic Association; Spring Meeting*: Berkeley, CA, USA, 1974; p. 137.
27. Nakayama, Y.; Baba, Y.; Yasuda, H.; Kawakita, K.; Ueyama, N. Stereospecific Polymerizations of Conjugated Dienes by Single Site Iron Complexes Having Chelating N,N,N-Donor Ligands. *Macromolecules* **2003**, *36*, 7953–7958. [[CrossRef](#)]
28. Kazakov, I.V.; Bodensteiner, M.; Timoshkin, A.Y. Masking of Lewis acidity trends in the solid-state structures of trichlorido- and tribromido(2,2':6',2''-terpyridine- κ^3N,N',N'')gallium(III). *Acta Crystallogr. Sect. C* **2014**, *70*, 312–313. [[CrossRef](#)]
29. Butcher, R.J.; George, C.; Muratore, N.; Purdy, A.P. Trichloro(2,6-di-2-pyridylpyridine- κ^3N)indium(III). *Acta Crystallogr. Sect. E* **2003**, *59*, m1107–m1109. [[CrossRef](#)]
30. Zhang, Y.; Yuan, S.; Yuan, Y.; Bao, Y.; Ran, Q.; Liu, E.; Fan, J.; Li, W. Alleviation of π - π^* Transition Enabling Enhanced Luminescence in Emerging TpyInCl_x ($x = 3, 5$) Perovskite Single Crystals. *Adv. Opt. Mater.* **2022**, *10*, 2102041. [[CrossRef](#)]
31. Curnock, E.; Levason, W.; Light, M.E.; Luthra, S.K.; McRobbie, G.; Monzittu, F.M.; Reid, G.; Williams, R.N. Group 3 metal trihalide complexes with neutral N-donor ligands—Exploring their affinity towards fluoride. *Dalton Trans.* **2018**, *47*, 6059–6068. [[CrossRef](#)]
32. Mantel, C.; Chen, H.; Crabtree, R.H.; Brudvig, G.W.; Pécaut, J.; Collomb, M.-N.; Duboc, C. High-Spin Chloro Mononuclear Mn^{III} Complexes: A Multifrequency High-Field EPR Study. *ChemPhysChem* **2005**, *6*, 541–546. [[CrossRef](#)]
33. Cotton, S.A.; Franckevicius, V.; Fawcett, J. Syntheses and structures of iron(III) complexes of simple N-donor ligands. *Polyhedron* **2002**, *21*, 2055–2061. [[CrossRef](#)]
34. Paraskevopoulos, J.N.; Smith, P.J.; Hoppe, H.C.; Chopra, D.; Govender, T.; Kruger, H.G.; Maguire, G.E.M. Terpyridyl Complexes as Antimalarial Agents. *S. Afr. J. Chem.* **2013**, *66*, 80–85.
35. Laurent, F.; Plantalech, E.; Donnadiou, B.; Jiménez, A.; Hernández, F.; Martínez-Ripoll, M.; Biner, M.; Llobet, A. Synthesis, structure and redox properties of ruthenium complexes containing the tpm facial and the trpy meridional tridentate ligands. Crystal structures of [RuCl₃(trpy)] and [Ru(tpm)(py)₃](PF₆)₂. *Polyhedron* **1999**, *18*, 3321–3331. [[CrossRef](#)]
36. Dobroschke, M.; Geldmacher, Y.; Ott, I.; Harlos, M.; Kater, L.; Wagner, L.; Gust, R.; Sheldrick, W.S.; Prokop, A. Cytotoxic Rhodium(III) and Iridium(III) Polypyridyl Complexes: Structure–Activity Relationships, Antileukemic Activity, and Apoptosis Induction. *ChemMedChem* **2009**, *4*, 177–187. [[CrossRef](#)] [[PubMed](#)]
37. Demadis, K.D.; El-Samanody, E.-S.; Meyer, T.J.; White, P.S. Structural and redox chemistry of osmium(III) chloro complexes containing 2,2':6',2''-terpyridyl and tris-pyrazolyl borate ligands. *Polyhedron* **1999**, *18*, 1587–1594. [[CrossRef](#)]
38. Chong, J.; Besnard, C.; Cruz, C.M.; Pigué, C.; Jiménez, J.-R. Heteroleptic *mer*-[Cr(N[⊖]N[⊖]N)(CN)₃] complexes: Synthetic challenge, structural characterization and photophysical properties. *Dalton Trans.* **2022**, *51*, 4297–4309. [[CrossRef](#)]
39. Bhalla, R.; Levason, W.; Luthra, S.K.; McRobbie, G.; Monzittu, F.M.; Palmer, J.; Reid, G.; Sanderson, G.; Zhang, W. Hydrothermal synthesis of Group 13 metal trifluoride complexes with neutral N-donor ligands. *Dalton Trans.* **2015**, *44*, 9569–9580. [[CrossRef](#)]
40. Blower, P.J.; Levason, W.; Luthra, S.K.; McRobbie, G.; Monzittu, F.M.; Mules, T.O.; Reid, G.; Subhan, M.N. Exploring transition metal fluoride chelates—Synthesis, properties and prospects towards potential PET probes. *Dalton Trans.* **2019**, *48*, 6767–6776. [[CrossRef](#)]
41. Mantel, C.; Hassan, A.K.; Pécaut, J.; Deronzier, A.; Collomb, M.-N.; Duboc-Toia, C. A High-Frequency and High-Field EPR Study of New Azide and Fluoride Mononuclear Mn(III) Complexes. *J. Am. Chem. Soc.* **2003**, *125*, 12337–12344. [[CrossRef](#)]
42. Cloete, N.; Visser, H.G.; Roodt, A. *mer*-Trichloro(2,2',2''-terpyridine)chromium(III) dimethyl sulfoxide solvate. *Acta Crystallogr. Sect. E* **2007**, *63*, m45–m47. [[CrossRef](#)]
43. Pruchnik, F.P.; Jakimowicz, P.; Ciunik, Z.; Zakrzewska-Czerwińska, J.; Opolski, A.; Wietrzyk, J.; Wojdat, E. Rhodium(III) complexes with polypyridyls and pyrazole and their antitumor activity. *Inorg. Chim. Acta* **2002**, *334*, 59–66. [[CrossRef](#)]
44. Taylor, S.D.; Shingade, V.M.; Muvirimi, R.; Hicks, S.D.; Krause, J.A.; Connick, W.B. Spectroscopic Characterization of Platinum(IV) Terpyridyl Complexes. *Inorg. Chem.* **2019**, *58*, 16364–16371. [[CrossRef](#)]
45. Ayscue, R.L.; Vallet, V.; Bertke, J.A.; Réal, F.; Knope, K.E. Structure–Property Relationships in Photoluminescent Bismuth Halide Organic Hybrid Materials. *Inorg. Chem.* **2021**, *60*, 9727–9744. [[CrossRef](#)] [[PubMed](#)]
46. Kepert, C.J.; Weimin, L.; Skelton, B.W.; White, A.H. Structural Systematics of Rare Earth Complexes. V The Hydrated 1:1 Adducts of 2,2':6',2''-Terpyridine with the Lanthanoid(III) Chlorides. *Aust. J. Chem.* **1994**, *47*, 365–384. [[CrossRef](#)]
47. Waters, A.F.; White, A.H. Synthesis and Structural Systematics of Nitrogen Base Adducts of Group 2 Salts. X Some Mixed-Ligand Complexes of Group 2 Metal Halides with 2,2':6',2''-Terpyridine and Oxygen Donors. *Aust. J. Chem.* **1996**, *49*, 147–154. [[CrossRef](#)]
48. Adcock, A.K.; Ayscue, R.L.; Breuer, L.M.; Verwiél, C.P.; Marwitz, A.C.; Bertke, J.A.; Vallet, V.; Réal, F.; Knope, K.E. Synthesis and photoluminescence of three bismuth(III)-organic compounds bearing heterocyclic N-donor ligands. *Dalton Trans.* **2020**, *49*, 11756–11771. [[CrossRef](#)]
49. Aullón, G.; Bellamy, D.; Brammer, L.; Bruton, E.A.; Orpen, A.G. Metal-bound chlorine often accepts hydrogen bonds. *Chem. Commun.* **1998**, *6*, 653–654. [[CrossRef](#)]

Disclaimer/Publisher's Note: The statements, opinions and data contained in all publications are solely those of the individual author(s) and contributor(s) and not of MDPI and/or the editor(s). MDPI and/or the editor(s) disclaim responsibility for any injury to people or property resulting from any ideas, methods, instructions or products referred to in the content.